



## Performance of Vertically-Polarized, Half-Rhombic Antennas Fabricated with Direct-Write Technology

*Prepared by:*  
Yaakov Cohen  
Cheyanne Herbert

*Faculty Advisors:*  
Dr. Thomas Montoya  
REU Site Director, Department of Electrical and Computer Engineering

Mr. James Randle  
Director, SDSMT Direct Write Laboratory

Dr. Alfred Boysen  
Professor, Department of Humanities

*Program Information:*  
National Science Foundation  
Grant NSF #1359476

Research Experience for Undergraduates:  
Bringing Us Together, Improving Communications and Lives  
Summer 2014

South Dakota School of Mines and Technology  
501 E Saint Joseph Street  
Rapid City, SD 57701

# TABLE OF CONTENTS

Abstract .....	2
Introduction .....	2
Objectives .....	4
Broader Impact .....	5
Procedure .....	5
Antenna Materials .....	6
Fabrication Equipment .....	6
Construction .....	8
Testing .....	8
Results .....	13
Copper Wire Results .....	13
ECM CI-2002 Trace Results .....	17
Parelec Parmod VLT (AMA-300) Trace Results .....	18
Simulation Results.....	19
Discussion .....	23
Conclusion .....	25
References .....	25
Acknowledgments .....	26

# **Abstract**

This study investigated the use of direct-write technology to construct vertically-polarized, half-rhombic antennas. By the Method of Images principle, these antennas perform like full-rhombic antennas. The antennas were fabricated with a material deposition printing system and from wire. The feed end of the antennas was connected to an SMA connector. A chip resistor was connected to the other end to terminate the antenna. The physical antennas were then compared to models generated with computer software.

## **1. Introduction**

Rhombic antennas were the one of the first high-frequency antennas designed for high directivity and functionality over a large range of frequencies, constructed by connecting two vee antennas together at their open ends (Martin-Caloto, 1). One vertex of a vee is the feed for the antenna, and the other vertex is connected on a terminating resistor, ranging from 600 to 800 Ohms (Blake, 219). This design (seen in (a) of Figure 1) produces an antenna that is nonresonant and unidirectional (Blake, 219).

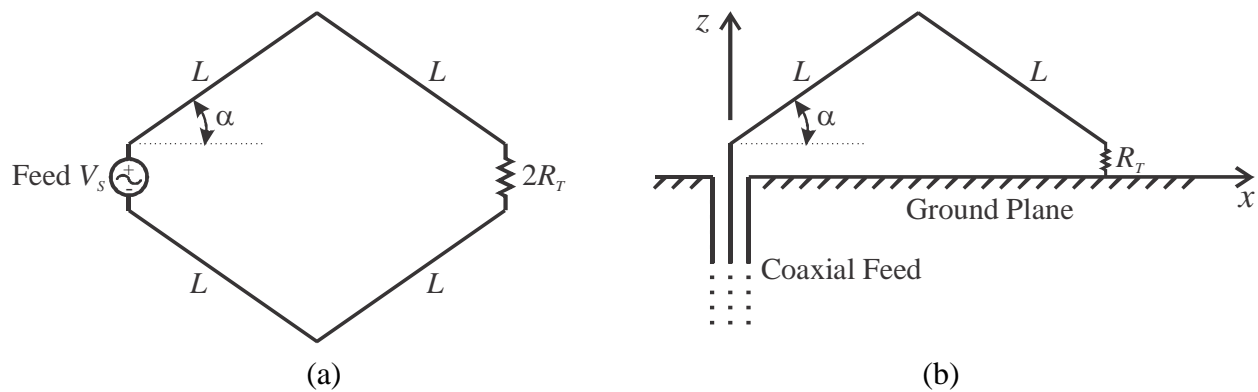


**Figure 1: A diagram of a full-rhombic (a) and half-rhombic (b) antenna.**

Rhombic antennas also have some limitations. According to Angel Martin-Caloto, from the Department of Electrical Engineering at Stanford University, “For proper performance, the individual legs of rhombic antennas must be several wavelengths long. At frequencies near the low end of the range employed for long-distance communication, this results in antennas of great size. A rhombic antenna designed to operate at a frequency of 4Mc, for example, might be more than 1000 feet long and 300 feet wide, requiring a land area of approximately 7 acres for installation.” (Martin-Caloto, 2). As a result, most early rhombic antennas were built parallel to the ground plane, e.g. horizontally-polarized. Optimum design equations have been studied for horizontally-polarized, full-rhombic antennas, but very little research has been directed towards vertically-polarized, half-rhombic antennas.

Half-rhombic antennas (seen in (b) of Figure 1) are designed differently, but function similarly to full-rhombic antennas because of the Method of Images (MOI) principle. The half-rhombic antenna is cut at the feed and resistor. Then, it is placed over a ground plane. Above the ground plane, the half-rhombic antenna exhibits the radiation patterns of a full-rhombic antenna while the input impedance is half that of a full-rhombic antenna. This is a consequence

of the MOI principle. The half-rhombic antennas studied in this research were also different from traditional rhombic antennas because of their orientation. Traditional rhombic antennas operated parallel to the ground plane, making them horizontally-polarized. In this research, the half-rhombic antennas were operated perpendicular to the ground plane, making them vertically-polarized (seen in Figure 2).

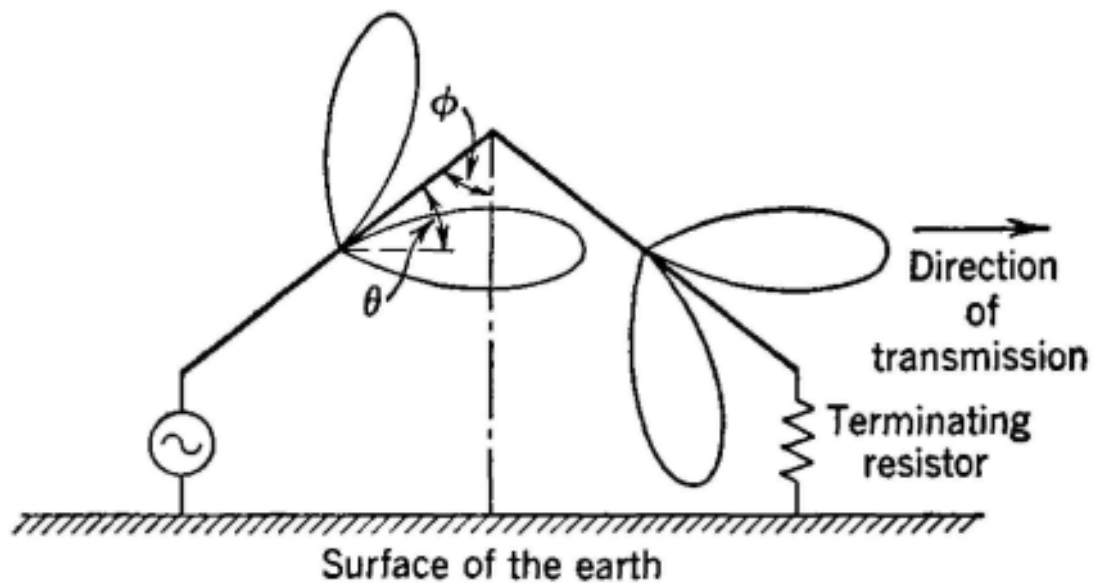


**Figure 2: A diagram of a vertically-polarized, half-rhombic antenna over a ground plane.**

## Objectives

Initially, this research studied vertically-polarized, half-rhombic antennas constructed using direct-write technology. The study focused on studying the performance changes if the included angle ( $\alpha$ ) in the Figure 1 and ( $\theta$ ) in Figure 2) and the terminating resistor values were varied. The  $S_{11}$  reflection coefficients and radiation patterns of the antennas were then compared to antennas with the same dimensions constructed with copper wire and simulated on a computer program.

To test the antenna performance, three different physical antenna types were constructed. Using direct-write technology and two separate conductive inks, two types of antenna traces were printed on flexible substrates. A final set of antennas was fabricated from copper wire. The results from the physical antennas were then compared to results from an antenna modeling software program.

This research had two primary goals:

1. To gather a base set of data for half-rhombic antenna impedance and radiation patterns for comparison to conductive traces, and for future research comparisons.
2. To fabricate half-rhombic antennas using direct-write technology and compare their performance to wire antennas and simulations.

## **2. Broader Impact**

This research was a proof of concept that direct-write technology can be used to accurately fabricate half-rhombic antennas. Direct-write technology offers significant advantages over traditional fabrication techniques. It is an inexpensive form of manufacturing, requiring only a substrate and an ink. Direct-write fabrication also offers easy design adaptability. Other manufacturing techniques can require expensive, wasteful, and sometimes costly changes to alter the design of an antenna. Designs for direct-write technology, however, can be changed in computer-aided design programs and ported directly to the deposition machine.

Printed antennas on flexible substrates have potential applications in virtually all fields that require wireless communication. Flexible antennas can be used in the military, biomedical industry, consumer electronics, and countless other applications.

### **3. Procedure**

This experiment was conducted with two classes of materials: conductive traces made from conductive ink and copper wire antennas. Each type of antenna required its own materials and construction procedure. However, a large portion of the equipment used and the testing procedure was similar for all antennas. This section will outline the steps taken in this experiment. Topics covered are:

- Antenna Materials
- Equipment
- Construction
- Testing

#### **Antenna Materials**

The antennas in this research were fabricated with three different materials. One set of antennas was constructed from copper wire. The second and third sets of antennas were fabricated with two different conductive inks.

Copper wire antennas were fabricated with coated and uncoated size 18 American Wire Gauge (AWG) wire. Half-Rhombic antennas require a terminating resistor to perform as traveling wave antennas. For this experiment, Mouser brand 0805 size surface chip resistors were used to terminate the antennas. The chips had nominal resistances of 300, 374, and 402 Ohms.

The first set of the conductive ink antennas were built using CI-2002, a carbon-based conductive ink manufactured by Engineered Conductive Materials, LLC. The second set was built with Parmod VLT (AMA-300), a silver-based conductive ink manufactured by Parelec Inc. The conductive traces were printed on KAPTON type HPP-ST, a plastic flexible substrate.

## **Fabrication Equipment**

### Copper Wire Antennas:

The equipment used to build copper wire antennas was limited to electronic calipers for taking measurements, and hand tools used to straighten, bend, and cut wire segments (e.g. pliers and wire cutters).

### Conductive Ink Antennas:

Using AutoCAD software, computer-aided design (CAD) files were constructed to model the desired antenna traces (i.e., draw the antenna). The CAD files were imported into a different software program, PathCAD. PathCAD is designed to work with the ink deposition system; it takes a drawing of the antenna/device and generates a script file with instructions for the deposition system on how to build that drawing. The script file specifies the three dimensional locations of the trace(s), and the direction and speed of movement for the ink deposition, and the air pressure (controls material flow) on the ink syringe at each point.

The script file was then sent to the ink deposition machine. In this experiment, an nScript 600-3Dn-HP (seen in Figure 3) located in the Direct Write Lab at SDSMT. The nScript machine deposits conductive ink from a syringe according to the instructions in the PathCAD script file. In this experiment, the conductive trace was deposited as a single continuous trace, with a constant air pressure applied to the syringe and the syringe held at a constant height above the Kapton substrate.

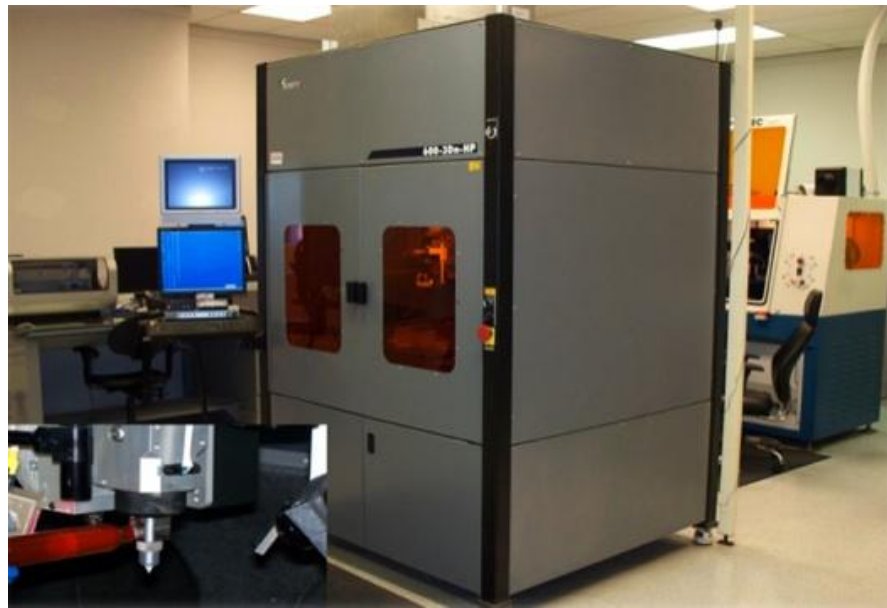


**Figure 3: A picture of the nScript 600-3Dn-HP machine in the Direct Write Lab.**

After the trace was printed on the substrate, it was thermally cured to solidify the ink, drive off existing solvents, and to achieve maximum conductivity. Curing was done in an Omegalux LMF-3550 oven also located in the Direct Write Lab.

### **Construction**

The rhombic antennas built for this research using conductive inks were designed the same leg lengths ( $L$ ), varying included angles ( $\alpha$ ) between sides, and multiple terminating

resistances. All antennas were fabricated to have leg lengths ( $L$ ) of 125 mm and a trace width of 1 mm. The included angles were varied in increments of  $5^\circ$  from  $30^\circ$  to  $45^\circ$ .

The width of any given trace must be measured experimentally. A variety of factors including temperature, humidity, and the exact viscosity of the ink lead to different conditions for every ink deposition. In this experiment, the goal was to achieve a 0.1 mm trace thickness. In order to construct antennas with this dimension, the input parameters on the nScrypt machine had to be adjusted and calibrated for every antenna. These parameters included deposition air pressure, axis movement speed, transition speed, and lift-off speed for the syringe.

After the traces were printed, they were cured in the Omegalux oven. For proper curing, oven temperature needed to increase slowly to the target temperature; this experiment used a  $5^\circ\text{C}$  increase per minute. The two inks used in this research were cured differently. The CI-2002 ink was cured at  $110^\circ\text{C}$  for 10 minutes while the Parmod VLT (AMA-300) ink was cured at  $140^\circ\text{C}$  for 5 minutes.

## **Testing**

This experiment used  $S_{11}$ /reflection coefficient measurements as the primary measurement for all antennas.  $S_{11}$  stands for scattering coefficient from port 1 back to port 1. In a multiport system, scattering refers to the energy received at a given port, given an input at another port. In a one port system, like an antenna,  $S_{11}$  refers to the energy received at port 1 given an input at port 1. In other words,  $S_{11}$  measures the energy reflected back from the antenna. The difference between the energy input and the reflection coefficient is the amount of energy radiated and released as heat from the antenna. Since most antennas are low loss systems,  $S_{11}$  can give a good approximation of the energy radiated from the antenna.

(Bevelacqua, 1)

Testing equipment in this experiment consisted of a Vector Network Analyzer (VNA), a copper ground plane, absorber blocks from an anechoic chamber (seen in Figure 4), and a 50 Ohm coaxial cable. The VNA in this experiment was an Agilent 4396B Network Analyzer designed to operate between 20 MHz and 1.82 GHz. The VNA was connected to an Agilent 85046A S-Parameter Test Set. The S-Parameter test set was connected to the coaxial cable using a 7.5mm to 3.5mm adapter. The coaxial was then connected to an SMA bulkhead connector mounted at the center of a ground plane. In this experiment, the ground plane measured 91.4 by 101.6 cm.

Before mounting the antenna, the VNA was calibrated using an Agilent 85033E 3.5mm Calibration Kit. The 50 Ohm coax was connected to the 3.5mm adapter, and then three attachments were made to the other end of the cable: a short circuit, an open circuit, and a known load. After calibration, the VNA adjusts itself to compensate for the coaxial cable and adapter (i.e., remove effects from measurements). Finally, a short circuit was applied between the bulkhead connector center conductor and the ground plane. An electrical delay on the VNA was then adjusted to compensate for the effect of the length of the bulkhead connector, allowing the  $S_{11}$  of only the antenna to be measured. At this point, the test setup was ready for the antenna to be mounted.

Each antenna material required its own mounting procedure on the ground plane. The copper wire antennas were soldered using a Weller WES51 soldering pen at 800 to 850 degrees Fahrenheit. The end of the feed side of the antenna was soldered to the top of the bulkhead connector between the antenna end and ground plane. On the terminating side, the terminating chip resistor was soldered to the ground plane. This is shown in Figure 4.

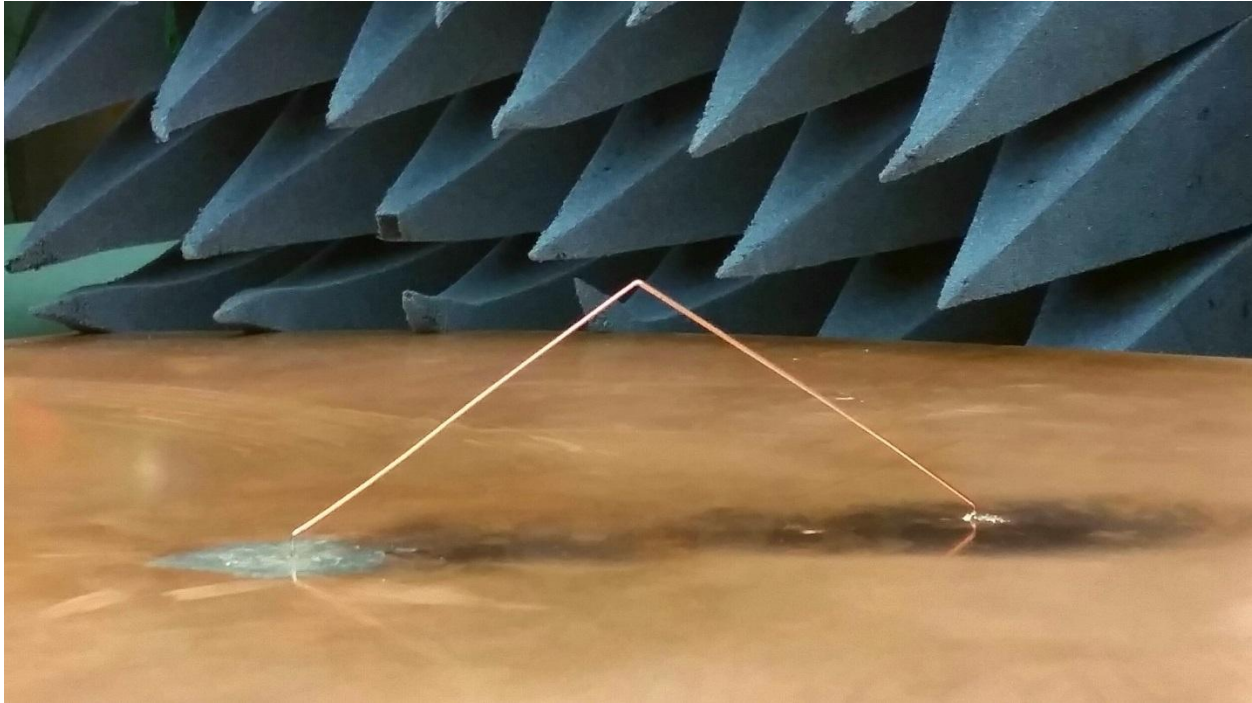


**Figure 4: A picture of the 35° copper wire antenna attached to the ground plane.**

The ink-based (ECM CI-2002) antenna was more difficult to mount. Both regular solder and a conductive solder paste would not adhere to the ECM trace. A partial solution was found which provided electrical conductivity, but little mechanical support. Additional ink was applied to the pin on the bulkhead connector, and along the feed stub of the trace. The two parts were pressed together and held in place with a wood block. The antenna was then cured to the connector using hot air from a TJ-70 Mini ThermoJet hand piece on an MBT PPS85A soldering and rework tool. This allowed the antenna to be cured in place (seen in Figure 5). However, in order to provide mechanical support to keep the antenna upright, Kapton supports were attached

to the back of the antenna using Scotch tape. No  $S_{11}$  testing was done on the Parelec antennas due to problems in making these connections.



**Figure 4: A picture of the 35° ink-based (CI-2002) antenna curing to the ground plane.**

The DC resistance of the antennas was measured with a two probe Temna 72-410A Digital Multimeter. Two measurements were taken for each antenna. The first measured resistance of the trace or wire alone, without a terminating resistor. The second measurement was taken after the terminating resistor was attached, and the antenna was mounted on the ground plane. This gave a measurement of the entire antenna resistance, and also ensured that the antenna was connected and that the solder was not acting as a short circuit around the terminating resistor.

After mounting each antenna, the ground plane was surrounded by blue foam absorbing blocks.  $S_{11}$  data was then measured and displayed on the VNA. An averaging factor of eight

was used for all data gathered.  $S_{11}$  was gathered at 601 frequency points between 20 MHz and 1.82 GHz (step size of 3 MHz). This means that all data recorded and displayed was an average of the previous 8 frequency sweeps of the VNA. Data was then saved graphically in a Smith Chart format (shows input impedance and  $S_{11}$ ), and numerically as an ASCII file with real and complex  $S_{11}$  values versus frequency.

Simulations were done using Numerical Electromagnetic Code Version 2 (NEC-2) software program, running in a Windows environment based on the Method of Moments (MOM) principle. Antennas were simulated to predict input impedance across a frequency range, and to determine radiation patterns. The simulation works by breaking the antenna up into discrete segments, and then calculating the current through each segment at the different frequencies. For simplicity, the antenna was modeled as a full-rhombic antenna without a ground plane, as though the antenna was in free space. By the MOI principle, output data can be related to the half-rhombic antennas. This is not a perfect simulation method, but it is a close approximation.

Output from the NEC program was used to create two types of graphs. Input impedance graphs were created in Microsoft Excel by dividing the simulation input impedance values by 2 to convert from those of a full-rhombic to a half-rhombic antenna, and then graphing the results versus frequency. Radiation pattern graphs were created by taking NEC output data (angle and power gain in dB) and running it through a script file in MATLAB to generate a polar graph.

Testing on physical antennas was done entirely between 20 MHz and 1.82 GHz. Initial simulations were done in this range as well; the simulations were extended up to 3.0 GHz.

## 4. Results

This section will cover the experimental and simulation results of this research. Specifically, it will cover:

- Copper wire antenna data, including physical dimensions, resistances, and  $S_{11}$  measurements
- ECM ink-based antenna trace data, including resistances and  $S_{11}$  measurements
- Parelec ink-based antenna trace resistances

### Copper Wire Results

Four copper wire (18 AWG) antennas were built for this experiment. The first antenna was made separately from the last three, both to compare tin-coated and uncoated wire, and to allow for comparison between uncoated wire antennas at different angles. Tin-coating will have essentially no impact on antenna performance. The four antennas, their angles, and their measurements, were as follows:

Antenna #	1	2	3	4
Angle (degrees)	35	30	35	40
Material	Tin coated copper	Uncoated copper	Uncoated copper	Uncoated copper
Feed Length (mm)	N/A	4.09	3.26	3.43
Main Side L1 (mm)	125.64	126.22	125.40	126.77
Main Side L2 (mm)	125.07	126.45	126.92	126.68
Terminating L (mm)	5.48	4.91	3.52	5.50
Average Wire Diameter (mm)	1.01	0.98	1.08	1.09

**Table 1: A table of the individual dimensions of the copper wire antennas.**

After soldering terminating resistors onto each antenna, its resistance was measured. The first antenna was tested only with a 374 Ohm terminating resistor. All 3 uncoated copper antennas were tested with 301, 374, and 402 Ohm terminating resistors. The resistances of the

wire portions of the antennas alone, with terminating resistors, and the measured values of the resistors alone were as follows:

Antenna #	1	2	3	4
Angle (degrees)	35	30	35	40
Wire Resistance (Ohm)	0.37	0.32	0.34	0.37
Antenna + 301 Ohm	N/A	297.7	297.9	297.7
Antenna + 374 Ohm	373.0	373.6	374.1	374.5
Antenna + 402 Ohm	N/A	401.4	400.8	400.5
301 Ohm Resistor Value	N/A	297.38	297.56	297.33
374 Ohm Resistor Value	372.63	373.28	373.76	374.13
402 Ohm Resistor Value	N/A	401.08	400.46	400.18

**Table 2: A table of the calculated resistance values for the copper wire antennas.**

Each antenna was then attached to the ground plane and connected to the VNA to measure the  $S_{11}$ /reflection coefficient data. The graphs that follow are input impedance of the antennas, calculated from the reflection coefficient data. Reflection coefficient is a complex value with both real and imaginary parts. Impedance also has a real and imaginary part, and is related to reflection coefficient, based on the characteristic impedance of the system. The VNA and cable in this experiment both have a characteristic impedance of 50 Ohms, and thus the equation relating the input impedance of an antenna to its  $S_{11}$ /Reflection coefficient is:

$$Z_{in} = Z_0 \frac{(1 + S_{11})}{(1 - S_{11})} = 50 \frac{(1 + S_{11})}{(1 - S_{11})}$$

Using this formula, the input impedance of each antenna as a function of frequency was calculated and graphed in Microsoft Excel. The graphs are grouped by antenna included angle and by terminating resistance. Angle grouped graphs show antennas with the same angle and varying resistance values. Resistance grouped graphs show antennas with the same resistance

and varying included angles. Each graph has two lines for each antenna, one for the real part of impedance, and one for the imaginary part.

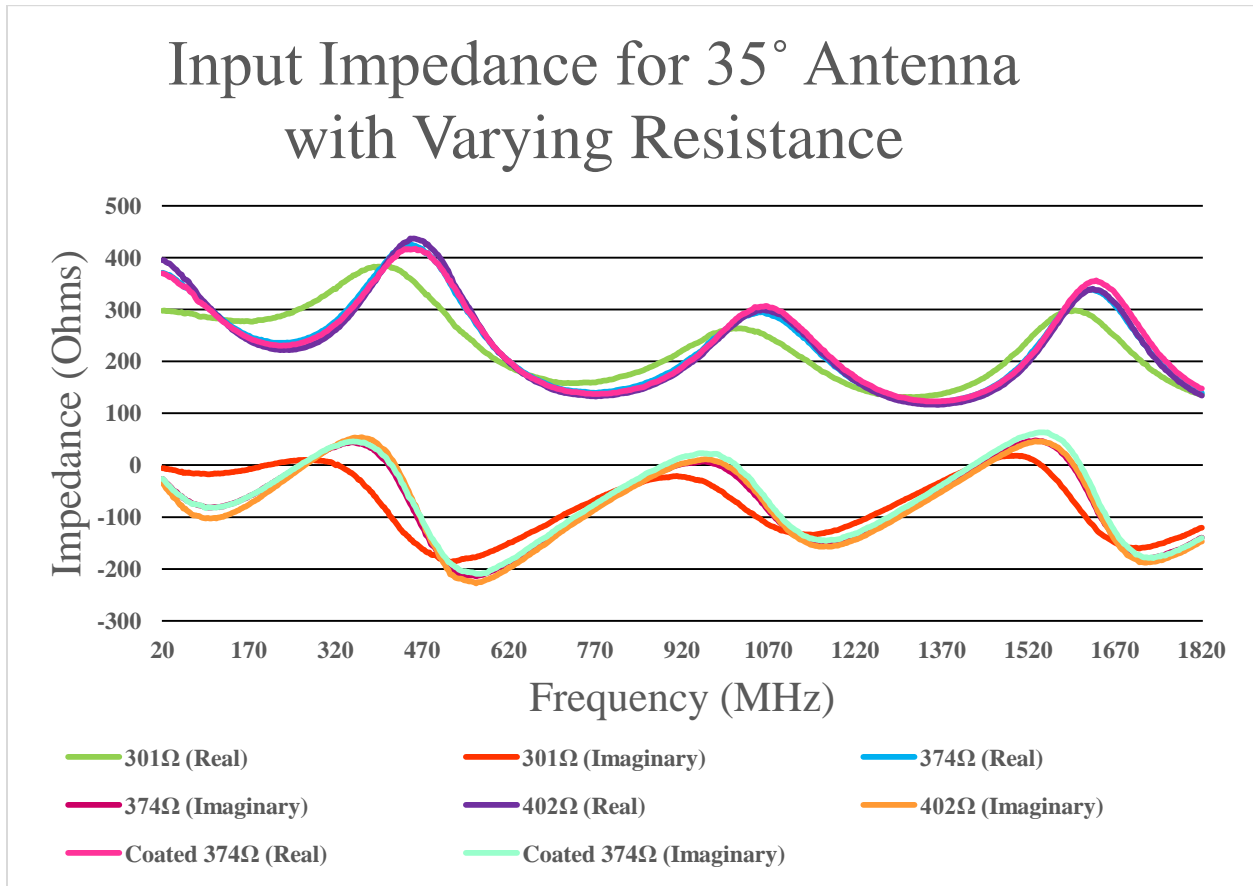


**Figure 6: A graph of the frequency response of 35 degree antennas with varying resistance.**

As seen in Figure 6, the response at 374 and 402 Ohms is very similar, while the 301 Ohm antenna shows a significantly shifted response with respect to frequency and in magnitude.

These results are very similar to results obtained for antennas with included angles of 30 and 40 degrees. The 374 and 402 Ohm antennas at those angles also show very similar curves, with the 301 Ohm curve again being shifted.

The tin-coated versus uncoated wire antennas with 374 Ohm terminations were nearly identical, both in magnitude and frequency response.

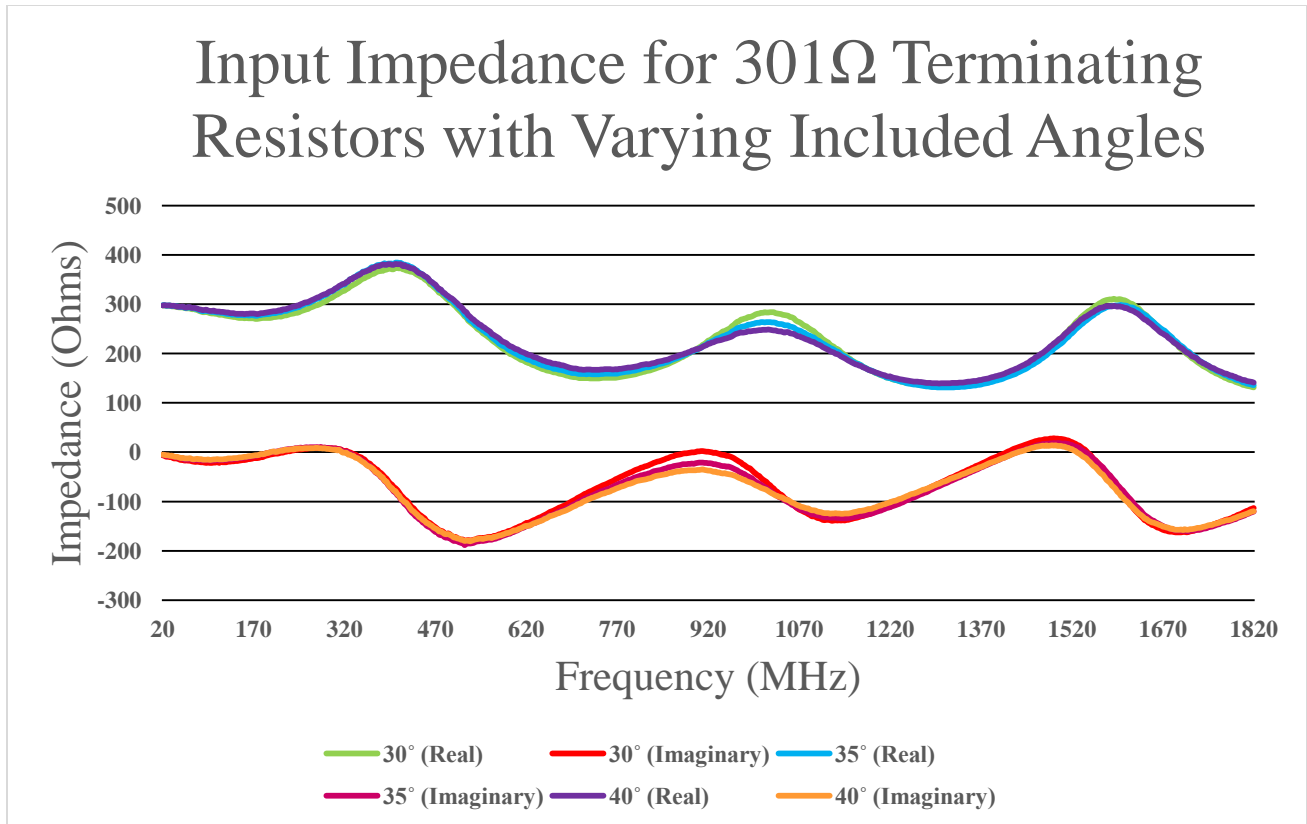


**Figure 7: A graph of the frequency response of antennas terminated with 301 Ohm resistors with varying included angles.**

As seen in Figure 7, varying the antenna angles with a constant terminating resistance had very minimal effect on impedance values. Antennas with different angles still reached very similar minimum impedance values at the same frequencies.

The following table lists the minimum real impedance values for all copper wire antennas, along with the frequencies at which they occur:

Angle	Resistance	Freq 1 (MHz)	Min Res ( $\Omega$ )	Freq 2 (MHz)	Min Res ( $\Omega$ )	Freq 3 (MHz)	Min Res ( $\Omega$ )
40°	301 $\Omega$	155	279.8	761	167.6	1301	139.3
40°	402 $\Omega$	245	224.1	770	141.0	1361	125.1
40°	374 $\Omega$	221	236.3	764	144.1	1343	125.5
30°	301 $\Omega$	173	270.0	728	149.4	1301	132.3
30°	402 $\Omega$	239	212.4	770	121.7	1352	111.6
30°	374 $\Omega$	224	225.4	761	125.3	1331	111.6
35°	301 $\Omega$	173	276.8	740	158.1	1322	131.2
35°	374 $\Omega$	224	235.5	770	139.1	1352	121.3
35°	402 $\Omega$	230	221.5	770	132.5	1361	116.4
35° *	374 $\Omega$	224	230.1	776	137.2	1352	122.7
* coated copper wire							

**Table 3: A table of the minimum real impedance values of the tested antennas.**

### ECM CI-2002 Trace Results

CI-2002 antennas were fabricated at 30, 35, 40, and 45 degree internal angles. However, after testing on the 35 degree antenna, it became apparent that the ink was not behaving conductively, and no more testing was done on this antenna. The first measurement taken on the 35 degree antenna was its DC resistance. The trace resistance was approximately 3700 Ohms, measured with a 2 probe DMM. With this large trace resistance, little current can be expected to flow on the antenna, large Ohmic losses can be anticipated (low efficiency), and minimal radiation can be expected. A decision was made to continue with  $S_{11}$  testing, to see whether any measurements could be taken. The following graph is the  $S_{11}$  data for the 35 degree ECM antenna:

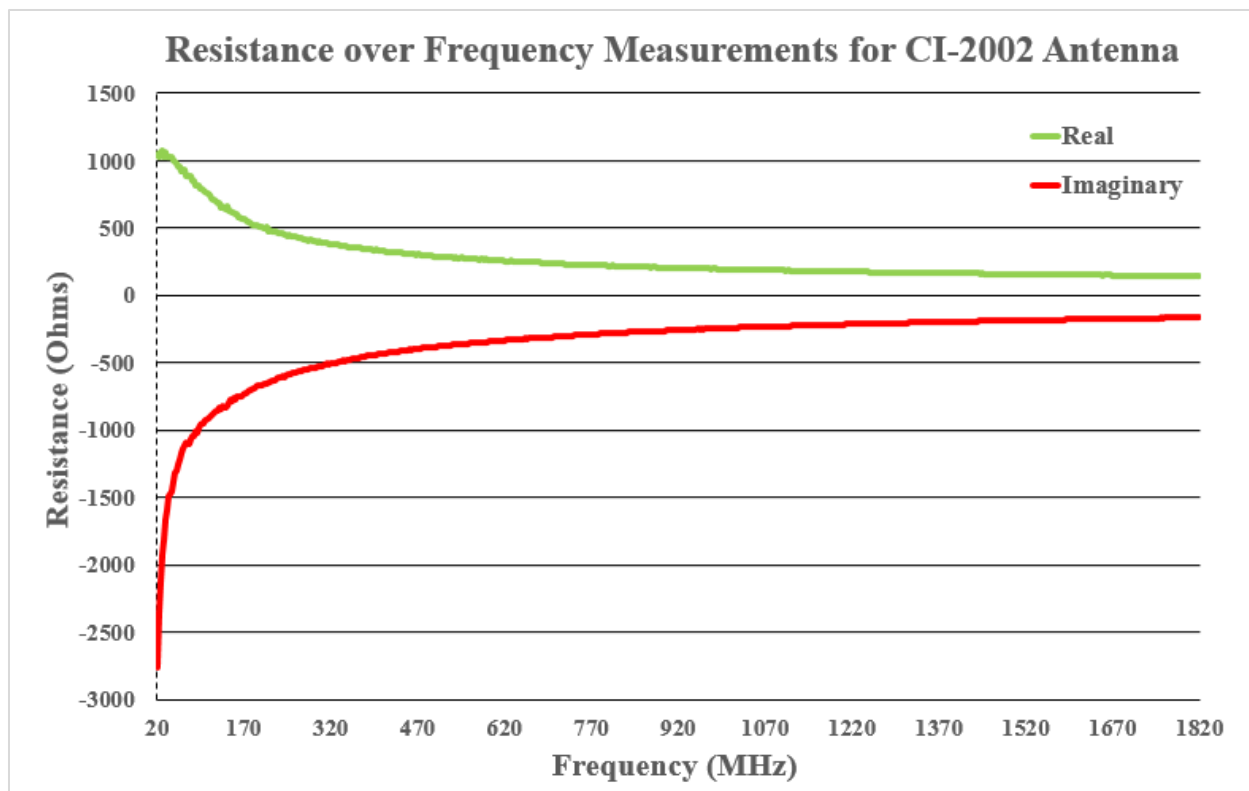


**Figure 8: A graph of the behavior of the 35 degree ink-based (CI-2002) antenna.**

Figure 8 shows that the trace is behaving more like a resistor than an antenna. It is believed that the ECM CI-2002 ink has gone bad while in storage (i.e., lost its conductive properties).

### **Parelec Parmod VLT (AMA-300) Trace Results**

The Parelec antennas were fabricated at 35 and 40 degrees. Initial resistance measurements were even worse than for the ECM antennas. Resistance was measured numerous times, with results varying from 150 Ohms per centimeter to an open circuit along the traces.

Both solder and solder paste would not adhere to the Parelec traces. The decision was made at this point not to continue testing, as behavior similar to the ECM trace, could be expected. It is believed that the Parelec Parmod VLT (AMA-300) ink has gone bad while in storage (i.e., lost its conductive properties).

## **Simulation Results**

Because the inks used did not produce conductive traces, the decision was made to simulate the copper wire antennas. The first round of simulation was done using the dimensions and resistance values obtained from the 35 degree uncoated copper wire antenna with a 301 Ohm terminating resistor.

A number of assumptions were made when setting up the antenna model for the simulation. First, the antenna was modeled as a full-rhombic antenna in free-space. Results were interpreted in light of the MOI principle to relate to the half-rhombic antennas over a ground plane. Second, the feed and terminating resistor segments were assumed to be of equal length and constant diameter. The terminating resistor value was doubled for the full-rhombic. Third, the radius of the wire was assumed to be constant, and equal to the 0.51 mm radius of 18 AWG wire. For comparison purposes, the copper wire results are presented on the same graph (seen in Figure 9).

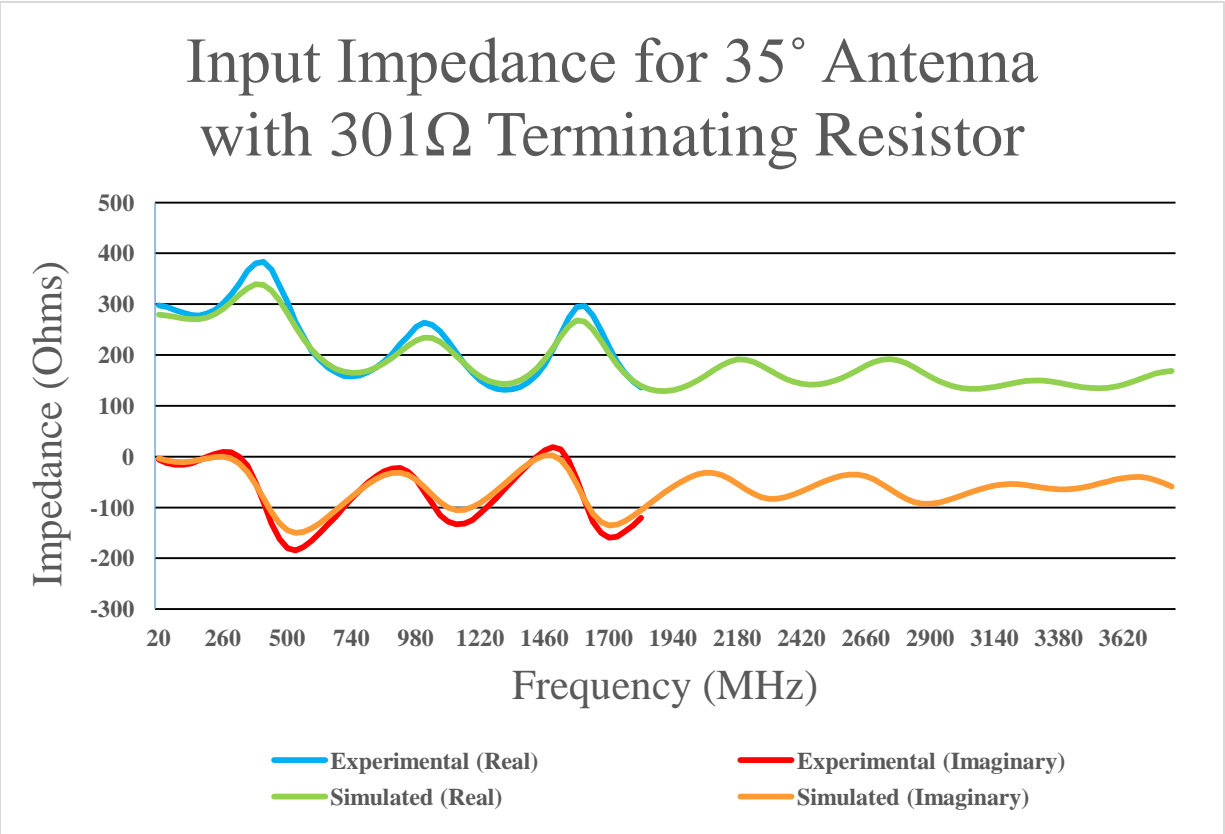


**Figure 9: A graph of the experimental and simulated data for the 35 degree antenna with the 301 Ohm terminating resistor. The simulations were run from 20 MHz to 3820 MHz.**

Finally, simulations were done to generate radiation patterns at selected frequencies. Radiation patterns changed as frequency increased. The following four graphs present the radiation patterns at the lowest and highest frequencies simulated. Note that there are two graphs for each frequency. In each case, the first graph is of the “E Plane,” which is effectively a side view of the antenna. The second graph is of the “H Plane” which is the view from above the antenna.

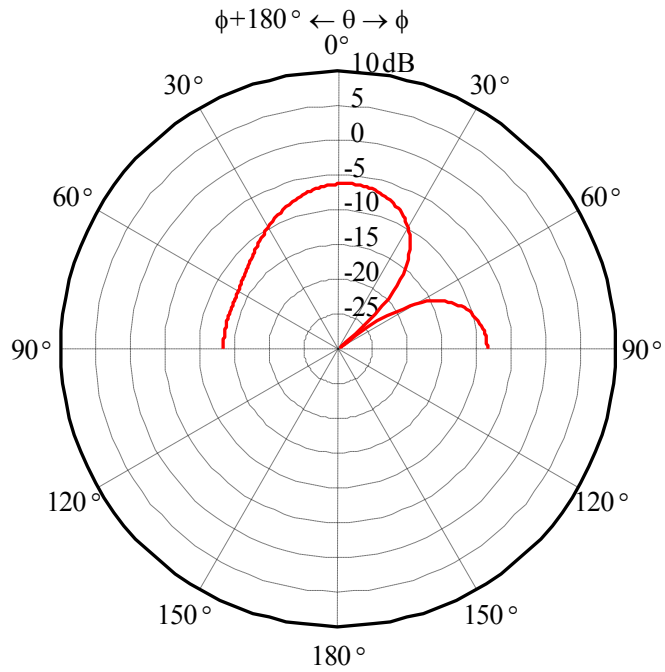


**Figure 10: E-Plane Power Gain Radiation Pattern for 35 degree half-rhombic antenna with 300 Ohm termination at 920 MHz ( $L \sim 126\text{mm} \sim 0.386\lambda$ ).**

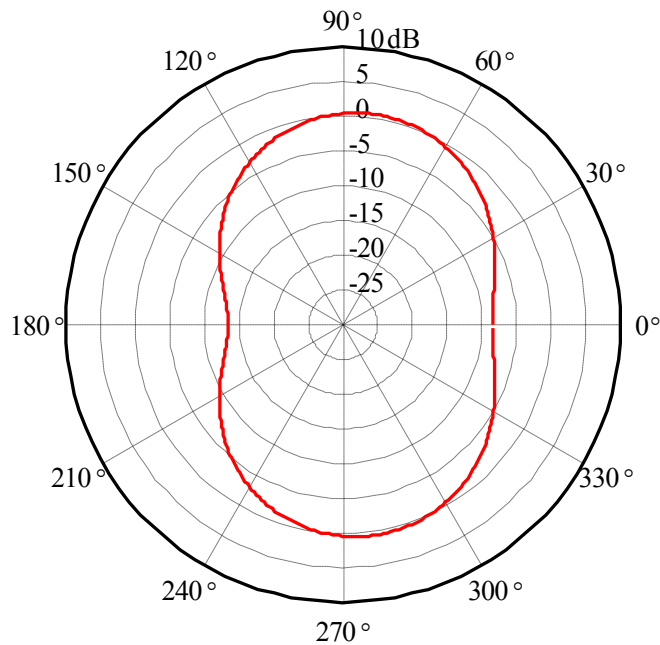


**Figure 11: H-Plane Power Gain Radiation Pattern for 35 degree half-rhombic antenna with 300 Ohm termination at 920 MHz ( $L \sim 126\text{mm} \sim 0.386\lambda$ ).**

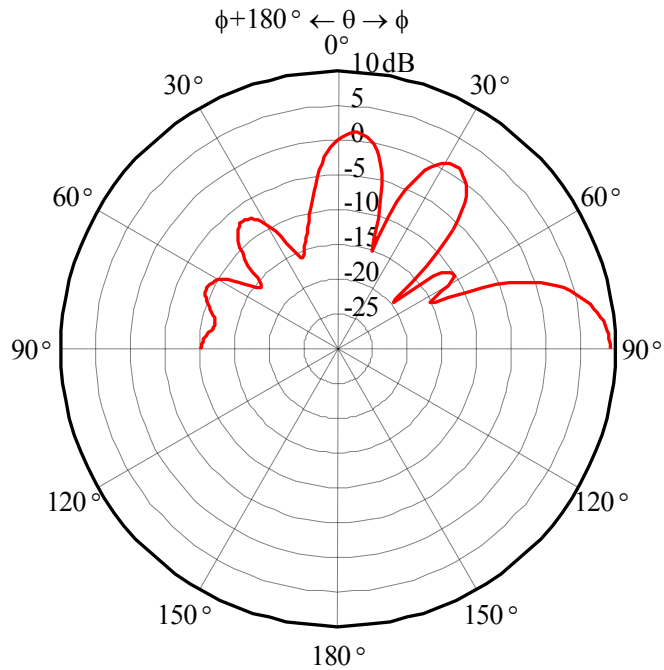


**Figure 12: E-Plane Power Gain Radiation Pattern for 35 degree half-rhombic antenna with 300 Ohm termination at 3500 MHz ( $L \sim 126\text{mm} \sim 1.47\lambda$ ).**

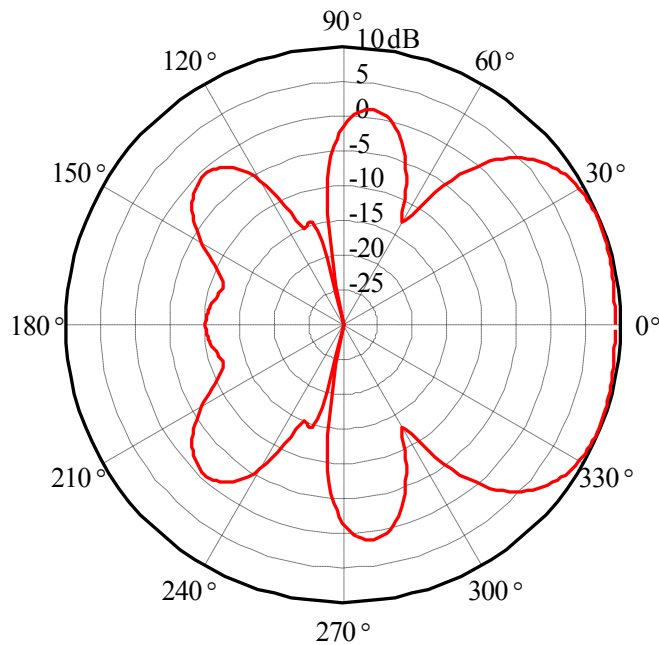


**Figure 13: H-Plane Power Gain Radiation Pattern for 35 degree half-rhombic antenna with 300 Ohm termination at 3500 MHz ( $L \sim 126\text{mm} \sim 1.47\lambda$ ).**

As can be seen, the antenna does not exhibit a directional radiation pattern pointed toward the terminating resistor at 920 MHz.

## 5. Discussion

This section will cover an analysis of the results for each type of antenna, and a comparison between the ink traces, the copper wire results, and the simulation.

Copper wire results were very close to what we expected. The antenna exhibits a decreasing real impedance as frequency increases. Unfortunately, when setting up this experiment insufficient consideration was given to the operating frequency of the antennas. When simulation was run at frequencies above those measurable on the VNA, the antenna displayed better radiation patterns, indicating that the best operating frequencies for these antennas was above the range measurable on the VNA. However, the data gathered in this experiment still provides a number of useful facts about copper wire half-rhombic antennas.

The most important conclusion drawn from this experiment is that terminating resistance affects antenna performance significantly more than included antenna angle for input impedance. Varying the terminating resistor from 301 to 374 to 402 Ohms significantly changed the impedance of the antenna. Additionally, changing the resistance also affected the exact frequency at which maximum and minimum impedances were achieved. Interestingly though, minimum impedance values did not seem to be significantly affected by changing the terminating resistance.

There is some margin of error for all low frequency measurements taken with the VNA. This is because the ground plane is relatively small compared to the in terms of wavelengths at low frequencies. Therefore, all measurements taken below approximately 200 MHz have

possible edge reflection errors. However, the general trend of data is similar both below and above 200 MHz, and, therefore, conclusions will be drawn from trends at all frequencies.

Overall, the copper wire antennas provide a good model for half-rhombic antenna behavior. Although the frequencies measured with the VNA appear to be below the optimum operating frequency of the antennas, the data gathered is still accurate for those lower frequencies, and can be compared to non-wire half-rhombic antennas.

Both the ECM and Parelec ink antennas were not conductive after curing. Consequently, although  $S_{11}$  data was measured for the ECM antenna, the resulting data is of no value because the ink did not demonstrate conductive properties. It is thought that the inks deteriorated with time (i.e., the conductive properties were changed).

Simulation of the copper wire antennas was highly successful. The simulated 35 degree 301 Ohm antenna impedance curve lined up extremely closely with the experimental data from the VNA. Both curves have the same rise and fall with frequencies, and reach the same minimum real impedance values. Because the curves are very similar up to 1.82 GHz, it is reasonable to infer that the simulation at higher frequencies is also accurate.

The simulation curve which extends to 3.82 GHz also validates the conclusion that the antennas are better suited to operate at higher frequency. As frequency passes above 2 GHz, maximum real impedance continues to drop, and appears to level off for the remainder of the simulation.

The radiation patterns from simulation give the best indication that the antennas would operate best at higher frequencies. At 920 MHz, almost no directivity is visible in either radiation plane. As frequency increases, the simulation shows greater directivity in both planes. In the E-plane, additional lobes develop, and by 3820 MHz there is a highly directive lobe with

about 9 dB of gain. In the H-plane, the radiation pattern changes from no directivity at 920 MHz to a large lobe with about dB of gain at 3820 MHz.

Overall, the simulation and copper wire experimental results agree quite well, and provide a good model and introductory set of data for future half-rhombic antenna testing, particularly at low frequencies.

## 6. Conclusion

This experiment succeeded in gathering good data on half-rhombic antennas. Copper wire antennas and simulation results provide an excellent dataset for future research, and a framework in which to predict behavior of future antennas. Although this experiment did not meet the goal of printing a working half-rhombic antenna with direct-write technology, future work with new conductive inks hold great promise for success.

Further research is necessary to further both goals of this experiment. Additional testing can be done with existing 125mm leg-length antennas to extend the S11 and impedance results to higher frequencies. Direct-write fabrication using a new ink with both conductive and adhesive properties should produce an antenna that can be compared to the copper wire and simulation results.

## References

1. Bevelacqua, P. J. (2008). *S-Parameters*. Retrieved from Antenna Theory.
2. Blake, L., & Long, M. (2009). *Antennas - Fundamentals, Design, Measurement*. *SciTech Publishing*, 219.
3. Martin-Caloto, A. (1960). The Study of Possibilities for Improving Space Utilization and Performance of Rhombic Antennas. *Stanford University Order No. 6001368*.

## **Acknowledgments**

The funding for this research came from the National Science Foundation, under grant #1359476. The authors would like to thank REU site director Dr. Thomas Montoya for his direction and guidance, Direct Write Laboratory director Mr. James Randle for his assistance, Professor of English Dr. Alfred Boysen for his suggestions and assistance in preparing this paper, and all of the faculty and staff at SDSM&T and in the Direct Write Laboratory for their help. Finally, the authors would like to thank the fellow members of the REU for their friendship and support.